doi:10.1111/mmi.12700

Bacterial chemoreceptors of different length classes signal independently

M. Karina Herrera Seitz,[1] Vered Frank,[2] Diego A. Massazza,[1] Ady Vaknin[2] and Claudia A. Studdert[1]*

[1]*Instituto de Investigaciones Biológicas, Universidad Nacional de Mar del Plata, 7600, Mar del Plata, Buenos Aires, Argentina.*

[2]*Racah Institute of Physics, Hebrew University, 91904, Jerusalem, Israel.*

Summary

Bacterial chemoreceptors sense environmental stimuli and govern cell movement by transmitting the information to the flagellar motors. The highly conserved cytoplasmic domain of chemoreceptors consists in an alpha-helical hairpin that forms in the homodimer a coiled-coil four-helix bundle. Several classes of chemoreceptors that differ in the length of the coiled-coil structure were characterized. Many bacterial species code for chemoreceptors that belong to different classes, but how these receptors are organized and function in the same cell remains an open question. *E. coli* cells normally code for single class chemoreceptors that form extended arrays based on trimers of dimers interconnected by the coupling protein CheW and the kinase CheA. This structure promotes effective coupling between the different receptors in the modulation of the kinase activity. In this work, we engineered functional derivatives of the Tsr chemoreceptor of *E. coli* that mimic receptors whose cytoplasmic domain is longer by two heptads. We found that these long Tsr receptors did not efficiently mix with the native receptors and appeared to function independently. Our results suggest that the assembly of membrane-bound receptors of different specificities into mixed clusters is dictated by the length-class to which the receptors belong, ensuring cooperative function only between receptors of the same class.

Accepted 30 June, 2014. *For correspondence. E-mail studdert@mdp.edu.ar; Tel. (+54) 223 475 3030; Fax (+54) 223 472 4143.

Introduction

Motile bacteria use a highly conserved signalling pathway, which controls flagellar movement in response to external stimuli, to seek optimal environmental conditions. Chemoreceptors, also called MCPs for methyl-accepting chemotaxis proteins, control the activity of the associated kinase CheA, which in turn phosphorylates CheY. Binding of CheY-phosphate to the flagellar switch causes a change in the direction of rotation of flagella and thus random reorientation of the cell (Hazelbauer and Lai, 2010).

Membrane-bound chemoreceptors are homodimers that usually possess a periplasmic ligand-binding domain. The cytoplasmic region of the protein consists in a HAMP domain (found in a number of histidine kinases, adenylyl cyclases, MCPs and phosphatases), followed by a long α-helical hairpin that, in a dimer, forms a coiled-coil four-helix bundle (see Fig. 2). The hairpin is composed of three distinct subdomains. The methylation subdomain contains residues that are modified by the enzymes CheB (deamidase/methyl esterase) and CheR (methyl transferase), involved in adaptation to persistent stimuli. The protein interaction region mediates contacts between different dimers to form trimers of dimers and also with the small coupling protein CheW and the dimeric histidine kinase CheA. Finally, the coupling subdomain connects the methylation and protein interaction regions, and contains conserved glycine residues that form a hinge, seemingly essential for function (Coleman *et al.*, 2005).

The coiled-coil α-helical structure of the chemoreceptor cytoplasmic region is essential for proper signal propagation from the periplasmic domain to the cytoplasmic tip. The importance of this structure is highlighted by the peculiar evolutionary pattern of receptors. Insertion/deletions of seven-residue stretches (heptads) in both arms of the hairpin produced receptor classes that differ in the length (Alexander and Zhulin, 2007) but not in the structure of the domain (Kim *et al.*, 1999; Park *et al.*, 2006). Membrane-bound receptors from different length classes seem to share also their higher-order organization; in several bacterial species macromolecular assemblies that contain trimers of receptor dimers can be identified in cryoelectron tomographic studies as column-like densities, corresponding to the cytoplasmic hairpin, running perpendicularly between the cytoplasmic membrane and the so-called

basal plate, composed by the small coupling protein CheW and the dimeric CheA kinase (Briegel *et al.*, 2009).

E. coli possesses five different chemoreceptors of the 36H-length class, meaning that their cytoplasmic hairpins are formed by two arms of eighteen heptads each. These MCPs are able to form mixed trimers of dimers (Studdert and Parkinson, 2004) that are assembled together in a stable array (Studdert and Parkinson, 2005; Erbse and Falke, 2009). Collaborative signalling between receptors of different specificities within this array has been demonstrated by a number of different approaches (Sourjik and Wingreen, 2012). Some species, like *E. coli*, code for a single class of receptors, whereas other species code for receptors of different classes (Alexander and Zhulin, 2007). However, it is not known whether they are spatially or temporally separated in the cell. In this work, we report the construction of functional derivatives of the serine receptor Tsr whose cytoplasmic hairpins are longer by two heptads, mimicking receptors of the 40H-class, and characterize the organization and function of these 40H-class derivatives when coexpressed with native 36H-class receptors (see Fig. 1). Our results are consistent with the notion that receptor of different classes do not mix, and effectively function independently to control cell motility.

Results

Construction of Tsr derivatives with fourteen-residue symmetric insertions

An alignment between the conserved cytoplasmic domain of Tsr, the serine chemoreceptor of *E. coli* (36H-class), and PctApp, an amino acid receptor from *P. putida* (40H-class), shows the presence of two extra fourteen-residue stretches in this latter that are located symmetrically with respect to the hairpin turn (Herrera Seitz *et al.*, 2012). The insertions are located in the coupling subdomain, below the glycine hinge (Fig. 2).

In order to build a 40H-class Tsr derivative, we inserted the corresponding sequences of PctApp into each arm of the Tsr hairpin. The resulting construct, called TsrH18, is schematically shown in Fig. 2. When expressed in a cell that lacks any native receptor, TsrH18 was unable to mediate serine taxis, as assessed in soft agar plates (Fig. 3). However, random mutagenesis applied to this construct rendered two single-point mutants that recovered significant serine-sensing function (Fig. 3). The functional derivatives TsrH18.6 (TsrH18 T350A, Tsr numbering) and TsrH18.8 (TsrH18 with a T to A change in the inserted heptad VDTMEQS) originated serine rings that were 30–50% and 60–80% the size of that of Tsr respectively (Figs 3 and 7B). Both rescuing mutations were located in the coupling subdomain, near or within the insertions (Fig. 2).

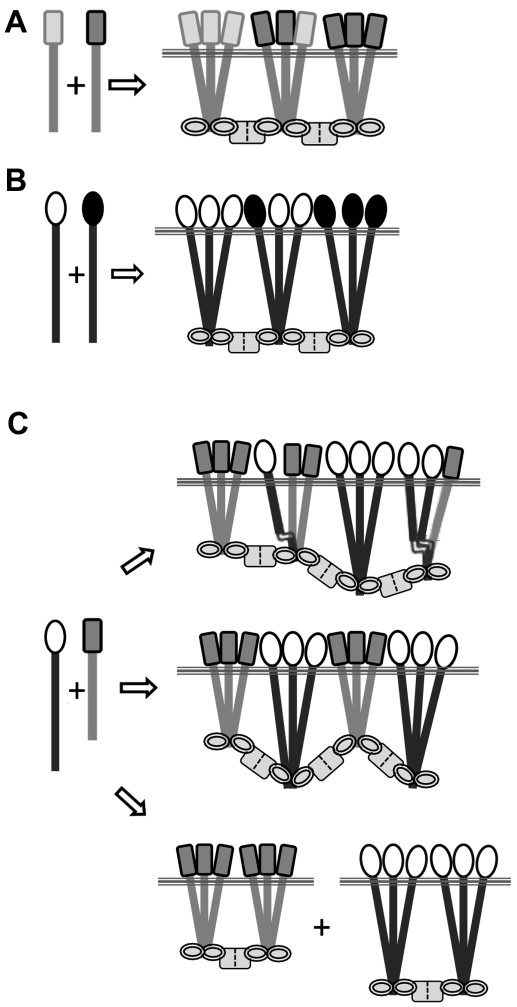

Fig. 1. Organization of chemoreceptor clusters containing receptors of different types. Receptor dimers are depicted as gray/black bars and differently shaded heads, representing the cytoplasmic and periplasmic domains respectively. Receptors belonging to the 36H-class are depicted as gray bars with rectangular heads; those belonging to the 40H-class, as longer black bars with oval heads. Head shading indicates specificity. The basal plate, formed by CheW (small oval) and dimeric CheA (rectangle), connects different trimers through their cytoplasmic tip.
A. Coexpressed 36H-class chemoreceptors form pure or mixed trimers that assemble into the same cluster.
B. Likewise, coexpressed 40H-class chemoreceptors form pure or mixed trimers that assemble together.
C. Three alternative organization possibilities for coexpressed receptors that belong to different classes are depicted: (*Top*) Pure or mixed trimers can form. The latter are probably distorted due to the constraints imposed by the cytoplasmic membrane and the basal plate. (*Middle*) Only pure trimers can form. As in the previous case, this results in a basal plate that is not parallel to the membrane. (*Bottom*) Pure trimers of different classes are segregated into separated clusters. Basal plates remain parallel to the cytoplasmic membrane.

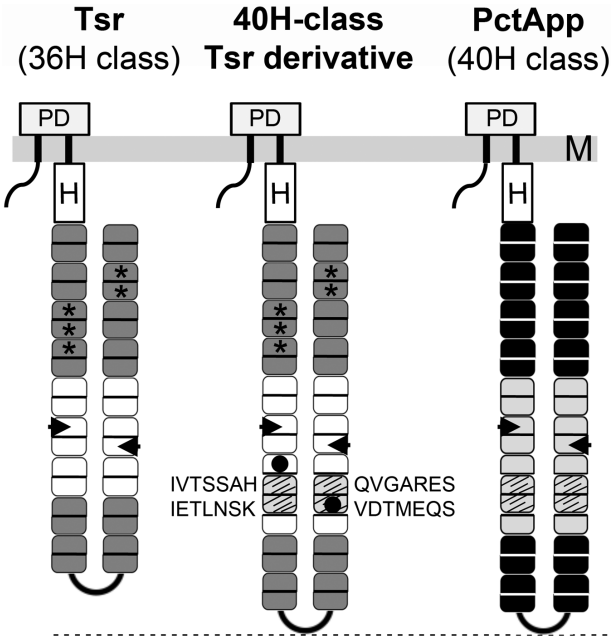

Fig. 2. Construction of 40H-class Tsr derivatives. Schematic representation of chemoreceptor monomers. M, plasma membrane; PD, periplasmic domain; H, HAMP domain. The cytoplasmic hairpin of Tsr is represented by 18 round-cornered squares, representing two heptads each (left, gray). The cytoplasmic hairpin of PctApp is represented by 20 round-cornered squares (right, black). In both receptors, colour intensity is used to indicate the three subdomains that form the signalling hairpin: the methylation/adaptation subdomain (membrane proximal, dark) contains the residues that are substrates of the modification enzymes (indicated by asterisks); the coupling subdomain (light) contains the glycine hinge (indicated by black arrowheads); the protein interaction subdomain (membrane distal, dark) contains the hairpin tip. To build a 40H-class Tsr derivative (TsrH18, middle), two heptads from each arm of PctApp cytoplasmic hairpin (striped regions) were introduced into the corresponding arms of Tsr hairpin. The corresponding sequences are indicated. Black filled circles indicate heptads where point mutations rendered functional derivatives (see text).

Kinase control by the 40H-class Tsr derivatives

CheY-phosphate generated by CheA activity binds to the flagellar switch and causes a change in the pattern of rotation of flagella from the default counterclockwise (CCW) direction to clockwise (CW). In the presence of attractant, cells exhibit CCW rotation because of kinase inhibition. We determined the ability of the 40H-class derivatives to control CheA activity by measuring the percentage of CW rotation observed upon expression of the different variants as the only receptor in the cell, as compared to wild-type Tsr. The response to the specific ligand was determined by measuring CW rotation immediately after the addition of a saturating amount of serine. In the presence of all the other chemotaxis proteins, all three 40H-class variants were able to activate the kinase, but only the functional derivatives TsrH18.6 and TsrH18.8 responded to the addition of serine with kinase inhibition (Fig. 4A, R+B+ strain).

In wild-type cells, kinase inhibition is transient, and the initial activity is recovered through an adaptation process mediated by the opposing activities of the deamidase/methyl esterase CheB and the methyl transferase CheR. The modification state of the receptors strongly affects their kinase control properties; the highly methylated form is more active and less sensitive than the completely demethylated form. Two of the methylation sites are made as glutamines but converted to glutamates by the deamidase CheB. We examined the kinase control ability of the 40H-class Tsr derivatives in strains lacking one or both modification enzymes (Fig. 4A). All three 40H-class variants were able to activate the kinase, and the original construct TsrH18 remained unresponsive to serine, in all backgrounds. The functional derivative TsrH18.8 became blind to serine in strains lacking CheB suggesting that, in this construct, deamidation of the glutamine residues involved in adaptation is essential for an appropriate response to the attractant stimulus. The other functional derivative, TsrH18.6, did not loose its ability to respond to serine in any of the strains, resembling the behaviour of wild-type Tsr. We then chose this variant to study its organization in the cell and signalling properties when coexpressed with native *E. coli* receptors in subsequent experiments, performed in strains lacking the modification enzymes (see below). In order to compare the sensitivity to serine of TsrH18.6 with that of Tsr in these conditions, we used tethered cells to determine the serine concentration at which the percentage of CW rotation drops to fifty

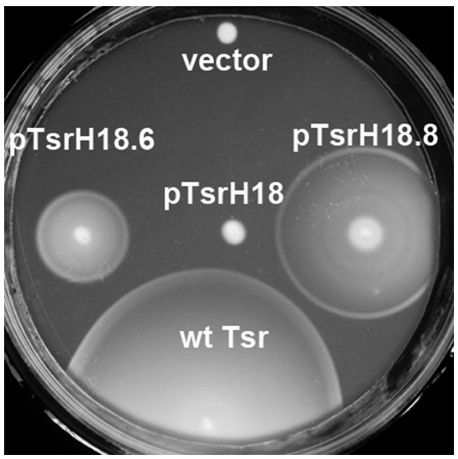

Fig. 3. Serine chemotaxis in semi-solid agar plates. UU2612 cells (lacking MCPs) carrying the control plasmid pKG116 (vector), pCS12 (wild-type Tsr) or pCS12 derivatives coding for the 40H-class Tsr variants (TsrH18, TsrH18.6 or TsrH18.8) were inoculated into semi-solid T-agar plates containing 12.5 μg ml^{-1} chloramphenicol and 0.45 μM sodium salicylate and incubated for 8–10 h at 30°C.

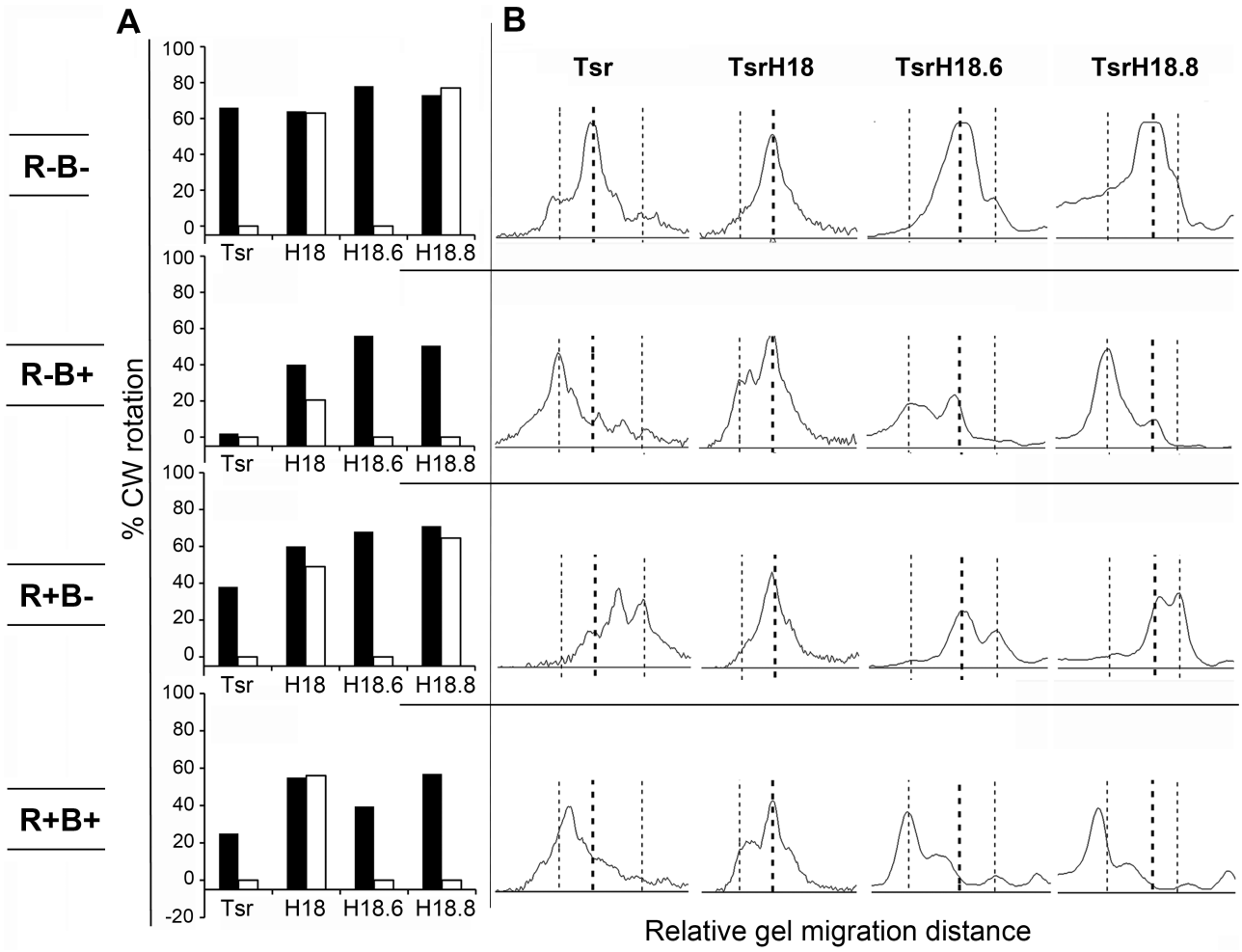

Fig. 4. Signalling abilities of 40H-class Tsr derivatives.
A. Receptor-mediated kinase control in different CheR/CheB backgrounds: The rotational behaviour of *E. coli* cells lacking native MCPs UU2612 (R+B+), UU2611 (R–B+), UU2632 (R+B–) or UU2610 (R–B–) expressing wild-type Tsr or the 40H-class derivatives was analysed in a tethering assay. Receptor expression was induced at physiological levels (0.45 μM sodium salicylate). Cells were observed in the absence of stimulus (black bars) or in the presence of 10 mM L-serine (white bars). The time that cells spend in CW rotation was calculated as described in Methods. In all cases, cells were observed within less than 3 min after the addition of attractant.
B. Basal modification state in different CheR/CheB backgrounds. Protein lysates from cells used in A were analysed in low bisacrylamide SDS-PAGE gels and visualized by immunoblotting using an anti-Tsr antiserum. The positions of the bands were determined by densitometry (ImageJ software). A vertical dashed line, bold, indicates the position of the unmodified receptor (R–B– strain). To facilitate comparison, vertical dashed lines indicate the position of the slowest migrating form of each receptor (i.e. the less modified) as well as the fastest migrating one (i.e. the more methylated form).

percent of that in the absence of stimulus. In the R–B– strain, the K½ for TsrH18.6 was higher than 100 μM serine, as compared with the value of 17 μM serine for wild-type Tsr previously determined by the same method (Herrera Seitz *et al.*, 2012), indicating that this 40H-class derivative is at least five times less sensitive to the attractant. This difference in sensitivity was also confirmed by FRET experiments carried out in cells expressing the individual receptors.

The variations in the modification state of Tsr in different background strains lacking one or both modification enzymes can be detected by their differential mobility in polyacrylamide gels that contain low-bisacrylamide (Fig. 4B, first column). The mobility of the TsrH18 derivative was almost the same in all the modification backgrounds (Fig. 4B, second column), indicating that this variant is a poor substrate for both enzymes; however, both TsrH18.6 and TsrH18.8 exhibited clear changes in their mobility depending on whether the background strain had CheR or CheB (Fig. 4B, last two columns). We conclude that the mutations present in the functional 40H-class derivatives render them a proper substrate for the modification enzymes. However, whereas TsrH18.6 is able to respond to attractant in any modification state, TsrH18.8 only

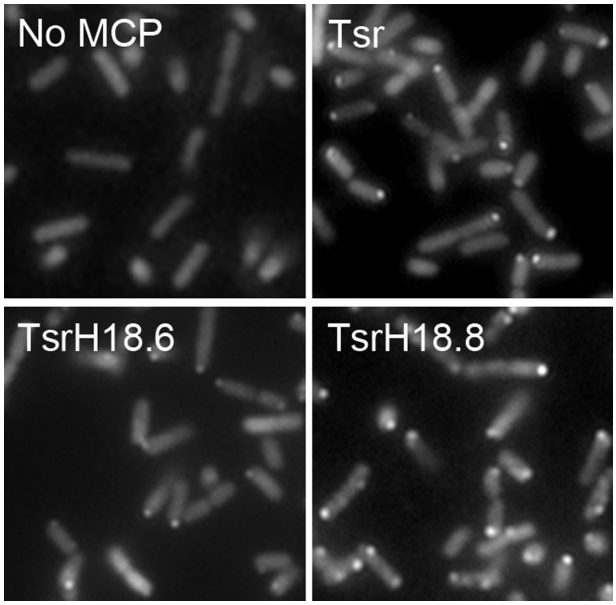

Fig. 5. Polar localization of 40H-class Tsr derivatives. Fluorescence images of *E. coli* cells coding for no MCP (strain MDP31), wild-type Tsr (strain MDP34), TsrH18.8 (strain MDP33) or TsrH18.6 (strain MDP32) and expressing CheA–YFP are shown.

responds to serine in the deamidated form generated by CheB (Fig. 4A). Furthermore, both TsrH18.6 and TsrH18.8 show proper localization when assessed using CheA–YFP as a reporter (Fig. 5). Polar clusters are clearly detected, though in TsrH18.6 they seem to be smaller than those observed for wild-type Tsr.

Coexpression of 40H-class Tsr derivatives and native (36H-class) receptors

Coexpression of the longer Tsr derivatives in *E. coli* cells together with native Tar receptors could result in three different receptor arrangements, schematically depicted in Fig. 1C. The two types of receptors could form mixed trimers of dimers (Fig. 1C, right, top panel). If this were the case, some kind of distortion of the longer receptor is anticipated, since the contact between the two dimers of different lengths should occur at the tip of the hairpin, a region that was not altered in our constructs. Alternatively, the two types of receptors could form separated homo-trimers of dimers with the two types of trimers assembled either into a common cluster (Fig. 1C, right, middle panel) or into separate clusters (Fig. 1C, right, bottom panel). To distinguish between these possibilities, we carried out the following experiments.

To assess the formation of mixed trimers, we examined the ability of the 40H-class Tsr derivatives to form mixed trimers with the native Tar receptor by using the cross-linking competition assay (Studdert and Parkinson, 2005). This assay uses a strain that harbours a chromosomal copy of the Tar receptor with a cysteine substitution at position 364 and is a target of the trifunctional cross-linker tris-(2-maleimidoethyl)-amine (TMEA). Highly expressed cysteine-less receptors that are incorporated into mixed trimers (competitors) significantly decrease the abundance of Tar-only trimers, and thus interfere with the formation of two- and three-subunit cross-linking products. Receptors that are not proficient in trimer formation (non-competitors) can thus be identified by their inability to interfere with the formation of cross-linking products. All three 40H-classTsr derivatives behaved as non-competitors (Fig. 6A), indicating that they were unable to efficiently incorporate into mixed trimers with Tar-S364C.

To assess the formation of functional mixed clusters, we used fluorescence anisotropy analysis of cells coexpressing Tar receptors tagged with yellow fluorescent protein (YFP) at their C-terminus and untagged long Tsr receptors. The polarization of the emitted fluorescence is sensitive in this case to changes in homo-FRET between the YFP fluorophores and thus to their relative proximity (Vaknin and Berg, 2007). In cells expressing Tar-YFP, fluorescence anisotropy is significantly reduced in the presence of CheA and CheW, condition that promotes strong clustering and consequently homo-FRET between different trimers of dimers (Frank and Vaknin, 2013). As seen in Fig. 6B, top panel, the incorporation of untagged Tsr receptors into the same cluster with Tar-YFP receptors effectively diluted the tag molecules in the cluster and thus increased the anisotropy level. This effect also led to a reduction in the magnitude of the change in anisotropy observed upon attractant stimuli (Fig. 6B, bottom panel). In contrast, no effect on the measured anisotropy or the response to α-methyl aspartate was detected when the 40H-class derivative TsrH18.6 was expressed together with Tar-YFP receptors (Fig. 6B). These findings support the previous conclusion that this longer variant is not incorporated into mixed trimers, and further suggest that the long-Tsr variant do not mix efficiently into the cluster formed by Tar receptors. It is worth noticing that the expression level of TsrH18.6 was lower than that of Tsr at the same concentration of inducer (Fig. S1). However, TsrH18.6 did not affect anisotropy at any level of expression, including protein levels that resulted in significant anisotropy changes for wild-type Tsr.

Functional consequences of coexpression of chemoreceptors belonging to the same or different class

In *E. coli*, both the sensitivity and the cooperativity of a chemoreceptor are affected by the presence of a receptor of different specificity (Sourjik and Berg, 2004). This coupling might rely on physical associations, through direct contact within mixed trimers of dimers and/or through the inter-connections provided by CheA and CheW (Vaknin

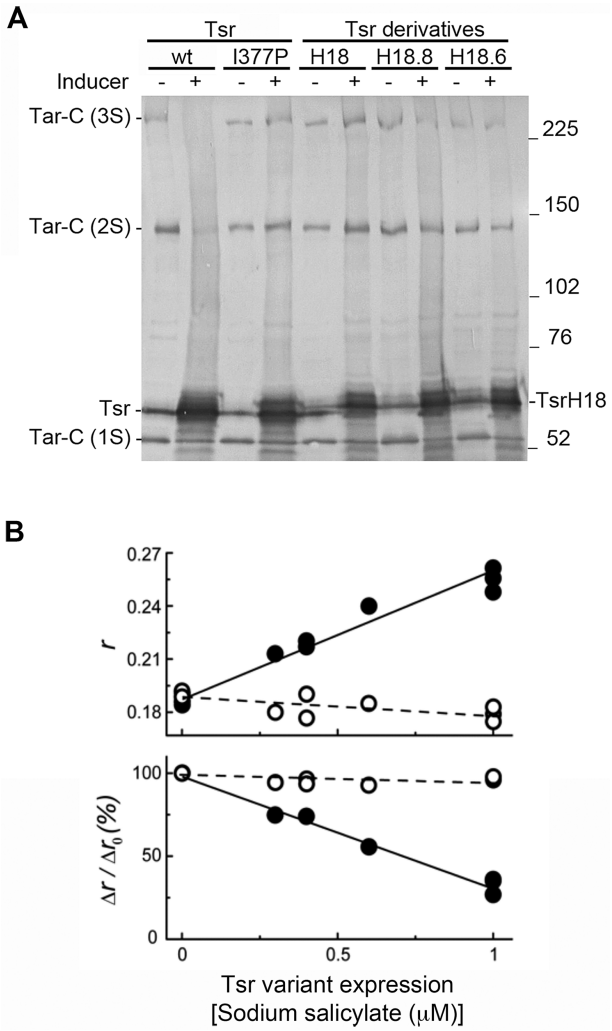

Fig. 6. Organization of coexpressed 40H-class Tsr derivatives and 36H-class Tar.
A. *In vivo* cross-linking assay for trimers of dimers. UU1613 cells (expressing Tar-S364C as the only MCP and lacking CheA, CheW and methylation enzymes) carrying plasmids that code for wild-type Tsr (wt), trimer deficient mutant Tsr I377P (I377P), or the 40H-class Tsr derivatives (TsrH18, TsrH18.6 or TsrH18.8) were induced at 0 (–) or 1.2 (+) μM sodium salicylate. Cells were treated with the tri-functional cross-linker TMEA as described in Methods. Protein lysates were analysed in low bisacrylamide SDS-PAGE gels and visualized by immunoblotting with anti-Tsr antibody. Molecular weight markers (kDa) are indicated on the right.
B. Fluorescence anisotropy of cells expressing Tar-YFP. The baseline anisotropy (top panel) and the relative response to 1 mM α-methylaspartate (bottom panel) is shown for VH1 cells expressing Tar-YFP and increasing amounts (induced by sodium salicylate) of either native Tsr (closed symbols) or TsrH18.6 (open symbols).

and Berg, 2008). We reasoned that the inability of the 40H-class receptors to mix with 36H-class native receptors should lead to the absence of coupling. To analyse whether the different-class receptors are able to signal collaboratively, we used a FRET-based assay to measure the fraction of CheA kinase activity that was controlled by saturating levels of the specific attractants when the two receptors were present at different ratios (Fig. 7A). Taking into account the lower level of expression of TsrH18.6 with respect to that of Tsr, we evaluated the actual Tar/Tsr variant ratios in these experiments. The obtained ratios reached 1.2 and 2.3 at the maximum induction level for the strains carrying Tsr or TsrH18.6 respectively (Fig. S2).

Kinase activity was determined by FRET-interactions between CheY–mCherry and CheZ–YFP, which are dependent on the level of CheY phosphorylation driven by CheA. The fraction of kinase activity inhibited by saturating α-methyl aspartate (Fig. 7A, top panel) or L-serine (Fig. 7A, middle panel) was measured relative to the activity inhibited by the presence of both aspartate and serine. In the absence of Tar induction, saturating serine controlled hundred per cent of kinase activity in the strains expressing wild-type Tsr or the 40H-class TsrH18.6, as expected. In both cases, as the level of Tar was progressively increased the fraction of CheA activity controlled by serine declined, with a concomitant increase of the fraction controlled by aspartate. In the strain carrying a chromosomal copy of Tsr, the sum of the responses toward aspartate and serine clearly exceeded the unit, indicating collaborative signalling (Fig. 7A, bottom panel, filled symbols). In contrast, the individual responses behaved additively and reached the unit in the strain expressing TsrH18.6 at all Tar/TsrH18.6 ratios (Fig. 7A, bottom panel, open symbols). This result is consistent with the lack of collaboration between the receptors from different length classes, suggesting that the 40H-class derivative is indeed assembled into an active complex that signals independently of the cluster conformed by 36H-class Tar receptors.

We had previously shown that the 40H-class amino acid receptor PctApp from *P. putida* does not form mixed trimers with Tar nor interferes with its function (Herrera Seitz *et al.*, 2012). We compared now the effect of PctApp or Tar expression on serine taxis in strains expressing wild-type Tsr or the 40H-class Tsr derivatives (Fig. 7B). Neither PctApp (40H) interfered with the serine-sensing function mediated by 36H-class Tsr, nor Tar (36H) affected the serine-sensing function mediated by 40H-class Tsr derivatives. However, PctApp expression caused a severe disruption of the serine ring in cells carrying the Tsr constructs that mimic receptors belonging to the same length class. Given the similarity between Tsr and its longer derivatives, the simplest explanation for the observed epistatic effect is the existence of interactions between the two different receptors of the same class, presumably through the formation of mixed trimers of dimers, rendering a non-functional complex. These interactions, however, do not seem to take place between PctApp and wild-type Tsr, whose cytoplasmic domain is shorter by two heptads. Thus, Tsr is able to assemble into a functional cluster that is not perturbed by the presence of PctApp.

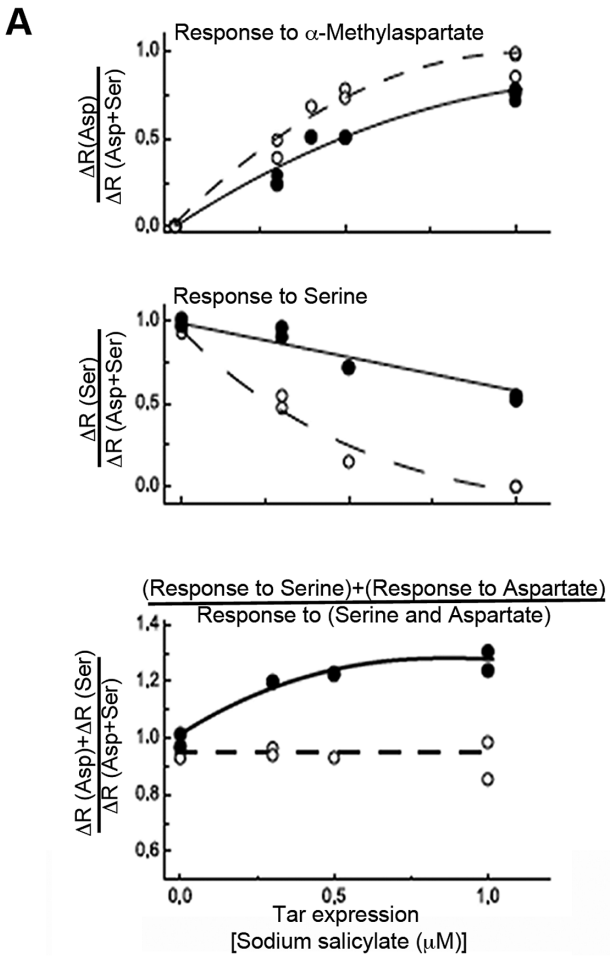

Fig. 7. Functional analysis of cells coexpressing receptors of the same or different class.
A. FRET-based analysis of kinase control. Cells expressing wild-type Tsr (filled symbols) or TsrH18.6 (open symbols) and increasing amounts of Tar (induced by sodium salicylate) were stimulated with 1 mM α-methyl aspartate (top) or 1 mM L-serine (middle), and the FRET response was measured as described in Methods. The results are normalized by the response to a mixture of serine and α-methyl aspartate at the same concentrations. The bottom graph represents the sum of the individual responses to α-methyl aspartate and L-serine.
B. Chemotaxis in semi-solid agar plates of cells carrying chromosome-coded wild-type Tsr (left), TsrH18.8 (middle) or TsrH18.8 (right) and no other receptor (top), plasmid-coded PctApp (middle) or Tar (bottom). Shaded labels indicate receptors of the 40H-class. Plasmid-coded receptors were induced at 0.45 μM sodium salicylate. Plates were incubated for 9 h at 30°C.

Discussion

The long Tsr chemoreceptor, with an addition of four complete turns of the α-helix on each arm of the Tsr cytoplasmic hairpin, was capable to assemble ternary complexes with CheW and CheA and activate the kinase, but failed to control it in response to serine and was a poor substrate for both CheR and CheB (Fig. 4A and B). However, both kinase control and substrate properties were significantly restored by two different single point mutations within the coupling subdomain, indicating that subtle alterations within the long hairpin cause radical changes in the signalling abilities of the protein. In TsrH18.6, the T350A mutation falls within a highly conserved socket, whose knob residue (M349′, holding an 'a' position in the heptad repeat) has been shown to be important for function in the homologous Tar receptor (Swain *et al.*, 2009). Similarly, in TsrH18.8 the T to A replacement in one of the inserted heptads also affects a socket structure that surrounds a conserved methionine knob (M536 in PctApp). Presumably, adjustments within these inter-helix connecting structures allow proper signal transmission along the enlarged hairpin. Moreover, the ability of the 40H-class functional derivative TsrH18.8 to control the kinase was dependent on CheB-mediated deamidation (Fig. 4A), highlighting the importance that helix interactions in the methylation region have on the ability of the coupling subdomain to transmit ligand information to the cytoplasmic tip (Swain *et al.*, 2009).

Even though the protein interaction region in our 40H-class functional constructs was unaltered, they were unable to form mixed trimer of dimers with 36H-class Tar (Fig. 6A), presumably due to the restricted length imposed by the membrane, the trimer contact region, and the allowed receptor tilt angle. The inability of the TsrH18.6 construct to alter the level of fluorescence anisotropy in a cell expressing Tar-YFP (Fig. 6B) further indicates that the 40H-class receptor is not efficiently incorporated into the Tar cluster. This also might be due to the restricted length imposed this time by the membrane and the need for common binding to CheA/W at the trimer contact region. This result agrees with the observation of clusters seemingly composed by a single type of receptor, based in the measured distances between the basal plate and the membrane, even in species that code for receptors belonging to different length-classes (Briegel *et al.*, 2009). Moreover, when coexpressed in cells, the different receptors were able to response to their specific ligands, but they were no longer able to signal in a collaborative fashion (Fig. 7A). Thus, different class receptors signal indepen-

dently in cells. Finally, we showed that the expression of PctApp, a 40H-class natural receptor from *P. putida*, does not interfere with wild-type Tsr function, whereas it has a strong epistatic effect on 40H-class Tsr derivatives, presumably by direct interaction within mixed trimers of dimers.

Independent clustering of receptors has been described in *Rhodobacter sphaeroides* (Wadhams *et al*., 2005) and in *Pseudomonas aeruginosa* (Guvener *et al*., 2006); in both cases one of the clusters involves a soluble MCP, belonging to a different length class than that to which the membrane-bound receptors belong. To our knowledge, this is the first report showing that two different membrane-bound receptors are unable to efficiently mix or be functionally coupled due to a difference in the length of their cytoplasmic domains.

Many bacterial species code for a large number of chemoreceptors, and it has been suggested that this number is related to the complexity of the environment the organisms have to cope with (Lacal *et al*., 2010). In a number of cases, the repertoire of MCPs includes representatives of different length classes (Alexander and Zhulin, 2007). Our results suggest that by utilizing different class sensors bacterial cells can control their functional cooperation.

Experimental procedures

Bacterial strains and plasmids

Strains were derivatives of the *E. coli* K12 strain RP437 (Parkinson and Houts, 1982) and are listed in Table S1. For tethered-cell, cross-linking, anisotropy or FRET assays, cells grown to mid-log phase on tryptone broth (1% tryptone, 0.5% sodium chloride) supplemented with the appropriate antibiotics/inducers were used. Plasmids used are listed in Table S2.

Construction of the 40H-class Tsr derivatives

Fourteen-residue insertions were introduced into the signalling domain of Tsr (see Fig. 2) through QuikChange Site-Directed Mutagenesis (Stratagene) using wild-type Tsr-coding plasmid pCS12 as template. Oligonucleotide primers used are listed in Table S3. The insertions were placed immediately after residues 357 and 424 in Tsr. Candidate mutants were verified by sequencing the entire protein-coding region. Variants carrying point mutations that suppressed the chemotaxis defects exhibited by the TsrH18 original construct were isolated as described in Massazza *et al.* (2012).

Semisolid agar plates for chemotaxis

Cells were inoculated into tryptone semisolid agar plates (Parkinson, 1976) containing 12.5 μg ml^{-1} chloramphenicol and 0.45–0.6 μM of sodium salicylate inducer. Plates were incubated at 30°C for 8–10 h.

Tethered-cell rotation assay

Flagellar rotation patterns were measured by cell tethering essentially as described (Parkinson, 1976), in the absence or presence of serine. Rotation profiles of cell populations were converted to CW time as described (Ames *et al*., 2002).

Protein expression and immunoblotting

Cells grown to mid-log phase on tryptone broth in the presence of the appropriate antibiotics/inducers were pelleted, washed, resuspended at OD = 20 in sample buffer (Laemmli, 1970) and lysed by boiling. Lysate proteins were analysed by SDS-PAGE as described (Feng *et al*., 1997) and visualized by immunoblotting with an antiserum that reacts with the highly conserved MCP signalling domain (Ames and Parkinson, 1994) as described (Herrera Seitz *et al*., 2012).

TMEA cross-linking competition assay for trimers of dimers

Cells carrying a chromosomal copy of *tar* gene with the S364C reporter substitution, and transformed with plasmids coding for the Tsr variants, were grown at 30°C to mid-log phase in tryptone broth containing 25 μg ml^{-1} chloramphenicol and 0 or 1.2 μM of sodium salicylate inducer. Cells were pelleted, harvested and treated as previously described (Studdert and Parkinson, 2004). Cells were pelleted, lysed, and analysed by SDS-PAGE and immunoblotting as described above.

Fluorescence polarization measurements

Fluorescence anisotropy of cells expressing Tar-YFP and increasing amounts of the Tsr variants was determined essentially as described in Frank and Vaknin (2013). Briefly, cells were grown to OD ~ 0.45, washed, resuspended in buffer (10 mM potassium phosphate, 0.1 mM EDTA, 1 mM methionine, 10 mM lactic acid, pH 7), immobilized on a coverslip and mounted in a gold-plated brass flow chamber in a Nikon FN1 microscope. The YFP proteins were excited with linearly polarized light using a linear glass polarizer. Fluorescence was collected using an FF01-542/27 emission filter and split using a polarizing beam-splitter cube. The steady-state polarization of the emitted fluorescence was represented by its fluorescence anisotropy r, defined as $(I_{par} - I_{per})/(I_{par} + 2I_{per})$, where I_{per} was corrected for any imperfections in the optical system.

FRET measurement of kinase activity

Changes in the kinase activity were detected by measuring changes in the level of FRET between CheY–mCherry and CheZ–YFP as described in Sourjik *et al.* (2007). Ratio, R, between the emissions in the red (630/75 nm) and yellow (550/50 nm) channels was monitored. Given the small changes in R (< 10%), the relative change in the fluorescence $\Delta R/R$ corresponds to the relative change in the number of CheY/CheZ pairs and thus the relative change in kinase activity.

Acknowledgements

We thank Sandy Parkinson (U. Utah) for providing strains and plasmids and for his continuous support, helpful discussions and specific comments about the figures presented in this manuscript. This work was supported by research grant PIP 0154 (to C.A.S. and K.H.S.) from the Consejo Nacional de Investigaciones Científicas y Técnicas (CONICET), Argentina and by the U.S.-Israel Binational Science Foundation. D.A.M. is a fellow from CONICET; K.H.S. and C.A.S. are CONICET Career Investigators.

References

Alexander, R.P., and Zhulin, I.B. (2007) Evolutionary genomics reveals conserved structural determinants of signaling and adaptation in microbial chemoreceptors. *Proc Natl Acad Sci USA* **104:** 2885–2890.

Ames, P., and Parkinson, J.S. (1994) Constitutively signaling fragments of Tsr, the *Escherichia coli* serine chemoreceptor. *J Bacteriol* **176:** 6340–6348.

Ames, P., Studdert, C.A., Reiser, R.H., and Parkinson, J.S. (2002) Collaborative signaling by mixed chemoreceptor teams in *Escherichia coli*. *Proc Natl Acad Sci USA* **99:** 7060–7065.

Briegel, A., Ortega D.R., Tocheva E.I., Wuichet K., Li Z., Chen S., *et al*. (2009) Universal architecture of bacterial chemoreceptor arrays. *Proc Natl Acad Sci USA* **106:** 17181–17186.

Coleman, M.D., Bass, R.B., Mehan, R.S., and Falke, J.J. (2005) Conserved glycine residues in the cytoplasmic domain of the aspartate receptor play essential roles in kinase coupling and on-off switching. *Biochemistry* **44:** 7687–7695.

Erbse, A.H., and Falke, J.J. (2009) The core signaling proteins of bacterial chemotaxis assemble to form an ultrastable complex. *Biochemistry* **48:** 6975–6987.

Feng, X., Baumgartner, J.W., and Hazelbauer, G.L. (1997) High- and low-abundance chemoreceptors in *Escherichia coli*: differential activities associated with closely related cytoplasmic domains. *J Bacteriol* **179:** 6714–6720.

Frank, V., and Vaknin, A. (2013) Prolonged stimuli alter the bacterial chemosensory clusters. *Mol Microbiol* **88:** 634–644.

Guvener, Z.T., Tifrea, D.F., and Harwood, C.S. (2006) Two different *Pseudomonas aeruginosa* chemosensory signal transduction complexes localize to cell poles and form and remould in stationary phase. *Mol Microbiol* **61:** 106–118.

Hazelbauer, G.L., and Lai, W.C. (2010) Bacterial chemoreceptors: providing enhanced features to two-component signaling. *Curr Opin Microbiol* **13:** 124–132.

Herrera Seitz, M.K., Soto, D., and Studdert, C.A. (2012) A chemoreceptor from *Pseudomonas putida* forms active signalling complexes in *Escherichia coli*. *Microbiology* **158:** 2283–2292.

Kim, K.K., Yokota, H., and Kim, S.H. (1999) Four-helical-bundle structure of the cytoplasmic domain of a serine chemotaxis receptor. *Nature* **400:** 787–792.

Lacal, J., Garcia-Fontana, C., Munoz-Martinez, F., Ramos, J.L., and Krell, T. (2010) Sensing of environmental signals: classification of chemoreceptors according to the size of their ligand binding regions. *Environ Microbiol* **12:** 2873–2884.

Laemmli, U.K. (1970) Cleavage of structural proteins during the assembly of the head of bacteriophage T4. *Nature* **227:** 680–685.

Massazza, D.A., Izzo, S.A., Gasperotti, A.F., Herrera Seitz, M.K., and Studdert, C.A. (2012) Functional and structural effects of seven-residue deletions on the coiled-coil cytoplasmic domain of a chemoreceptor. *Mol Microbiol* **83:** 224–239.

Park, S.Y., Borbat P.P., Gonzalez-Bonet G., Bhatnagar J., Pollard A.M., Freed J.H., *et al*. (2006) Reconstruction of the chemotaxis receptor-kinase assembly. *Nat Struct Mol Biol* **13:** 400–407.

Parkinson, J.S. (1976) *cheA*, *cheB*, and *cheC* genes of *Escherichia coli* and their role in chemotaxis. *J Bacteriol* **126:** 758–770.

Parkinson, J.S., and Houts, S.E. (1982) Isolation and behavior of *Escherichia coli* deletion mutants lacking chemotaxis functions. *J Bacteriol* **151:** 106–113.

Sourjik, V., and Berg, H.C. (2004) Functional interactions between receptors in bacterial chemotaxis. *Nature* **428:** 437–441.

Sourjik, V., and Wingreen, N.S. (2012) Responding to chemical gradients: bacterial chemotaxis. *Curr Opin Cell Biol* **24:** 262–268.

Sourjik, V., Vaknin, A., Shimizu, T.S., and Berg, H.C. (2007) *In vivo* measurement by FRET of pathway activity in bacterial chemotaxis. *Methods Enzymol* **423:** 365–391.

Studdert, C.A., and Parkinson, J.S. (2004) Crosslinking snapshots of bacterial chemoreceptor squads. *Proc Natl Acad Sci USA* **101:** 2117–2122.

Studdert, C.A., and Parkinson, J.S. (2005) Insights into the organization and dynamics of bacterial chemoreceptor clusters through *in vivo* crosslinking studies. *Proc Natl Acad Sci USA* **102:** 15623–15628.

Swain, K.E., Gonzalez, M.A., and Falke, J.J. (2009) Engineered socket study of signaling through a four-helix bundle: evidence for a yin-yang mechanism in the kinase control module of the aspartate receptor. *Biochemistry* **48:** 9266–9277.

Vaknin, A., and Berg, H.C. (2007) Physical responses of bacterial chemoreceptors. *J Mol Biol* **366:** 1416–1423.

Vaknin, A., and Berg, H.C. (2008) Direct evidence for coupling between bacterial chemoreceptors. *J Mol Biol* **382:** 573–577.

Wadhams, G.H., Martin, A.C., Warren, A.V., and Armitage, J.P. (2005) Requirements for chemotaxis protein localization in *Rhodobacter sphaeroides*. *Mol Microbiol* **58:** 895–902.

Supporting information

Additional supporting information may be found in the online version of this article at the publisher's web-site.